Europe PMC Funders Group
Author Manuscript
Arch Toxicol. Author manuscript; available in PMC 2017 October 24.

Published in final edited form as:
Arch Toxicol. 2017 May ; 91(5): 2245–2261. doi:10.1007/s00204-016-1885-6.

Inhibition of pannexin1 channels alleviates acetaminophen-induced hepatotoxicity

Michaël Maes[1], **Mitchell R. McGill**[2,#], **Tereza Cristina da Silva**[3], **Chloé Abels**[4,5], **Margitta Lebofsky**[2], **James L. Weemhoff**[2], **Taynã Tiburcio**[3], **Isabel Veloso Alves Pereira**[3], **Joost Willebrords**[1], **Sara Crespo Yanguas**[1], **Anwar Farhood**[6], **Alain Beschin**[4,5], **Jo A. Van Ginderachter**[4,5], **Silvia Penuela**[7], **Hartmut Jaeschke**[2], **Bruno Cogliati**[3,*], and **Mathieu Vinken**[1,*]

[1]Department of *In Vitro* Toxicology and Dermato-Cosmetology, Vrije Universiteit Brussel, Brussels, Belgium

[2]Department of Pharmacology, Toxicology and Therapeutics, University of Kansas Medical Center, Kansas City, United States of America

[3]Department of Pathology, School of Veterinary Medicine and Animal Science, University of São Paulo, São Paulo, Brazil

[4]Myeloid Cell Immunology Lab, VIB Inflammation Research Center, Ghent, Belgium

[5]Lab of Cellular and Molecular Immunology, Vrije Universiteit Brussel, Brussels, Belgium

[6]Department of Pathology, St. David's North Austin Medical Center, Austin, United States of America

[7]Department of Anatomy and Cell Biology, University of Western Ontario, London, Canada

Abstract

Background and aims—Pannexins constitute a relatively new family of transmembrane proteins that form channels linking the cytoplasmic compartment with the extracellular environment. Presence of pannexin1 in the liver has been documented previously, where it underlies inflammatory responses, such as those occurring upon ischemia-reperfusion injury. In the present study, we investigated whether pannexin1 plays a role in acute drug-induced liver toxicity.

Methods—Hepatic expression of pannexin1 was characterized in a mouse model of acetaminophen-induced hepatotoxicity. Subsequently, mice were overdosed with acetaminophen followed by treatment with the pannexin1 channel inhibitor ^{10}Panx1. Sampling was performed 1, 3, 6, 24 and 48 hours after acetaminophen administration. Evaluation of the effects of pannexin1

Corresponding author: Mathieu Vinken, Vrije Universiteit Brussel, Department of *In Vitro* Toxicology and Dermato-Cosmetology, Laarbeeklaan 103, B-1090 Brussels, Belgium; Tel: +32-2-4774587; Fax: +32-2-4774582; mvinken@vub.ac.be.
[#]Present address: Department of Pathology and Immunology, Washington University School of Medicine, St. Louis, United States of America.
[*]These authors share equal seniorship.

Conflict of interest: The authors declare that they have no conflict of interest.

Ethical approval: All applicable international, national, and/or institutional guidelines for the care and use of animals were followed.

Europe PMC Funders Author Manuscripts
Europe PMC Funders Author Manuscripts

Europe PMC Funders Author Manuscripts

channel inhibition was based on a number of clinically relevant read-outs, including protein adduct formation, measurement of aminotransferase activity and histopathological examination of liver tissue as well as on a series of markers of inflammation, oxidative stress and regeneration.

Results—Although no significant differences were found in histopathological analysis, pannexin1 channel inhibition reduced serum levels of alanine and aspartate aminotransferase. This was parallelled by a reduced amount of neutrophils recruited to the liver. Furthermore, alterations in the oxidized status were noticed with upregulation of glutathione levels upon suppression of pannexin1 channel opening. Concomitant promotion of regenerative activity was detected as judged on increased proliferating cell nuclear antigen protein quantities in ^{10}Panx1-treated mice.

Conclusions—Pannexin1 channels are important actors in liver injury triggered by acetaminophen. Inhibition of pannexin1 channel opening could represent a novel approach for the treatment of drug-induced hepatotoxicity.

Keywords

pannexin; hepatotoxicity; acetaminophen; cell death; inflammation; neutrophil

1 Introduction

Drug-induced liver injury is the leading cause of acute liver failure in Western countries with the vast majority being caused by overdosing with acetaminophen (APAP)/paracetamol, a readily available analgesic and antipyretic drug (Ichai and Samuel 2011; Lee 2008). APAP-induced hepatotoxicity depends on biotransformation mediated by cytochrome P450 2E1, yielding the deleterious metabolite *N*-acetyl-*p*-benzoquinone imine (NAPQI) (Dahlin et al. 1984). Under normal circumstances, NAPQI can be rapidly detoxified by binding to glutathione (GSH) (Dahlin et al. 1984). However, in case of APAP overdosing, GSH becomes depleted and NAPQI can react with protein sulfhydryl groups, which leads to the formation of protein adducts (Jollow et al. 1973; Mitchell et al. 1973). As a consequence, impaired mitochondrial respiration and oxidative stress are triggered associated with the onset of massive hepatocyte cell death and the induction of an inflammatory response. Indeed, elevated serum and liver concentrations of pro-inflammatory cytokines, and infiltrating neutrophils and monocytes are typically found in patients with fulminant hepatic failure (Blazka et al. 1995; Cover et al. 2006; Ishida et al. 2002; James et al. 2005; Lawson et al. 2000).

Pannexins are a relatively new family of transmembrane proteins that form channels connecting the cytosol with the extracellular environment. The pannexin family consists of 3 members (Panx1-3) of which 1 or more have been detected in every mammalian organ (Bruzzone et al. 2003; Le Vasseur et al. 2014; Penuela et al. 2007). A number of studies have reported the presence of Panx1 in liver, more specifically in hepatocytes and Kupffer cells (Bruzzone et al. 2003; Csak et al. 2011; Ganz et al. 2011; Kim et al. 2015; Sáez et al. 2014; Xiao et al. 2012). When open, Panx1 channels form transmembrane conduits allowing the passage of ions and hydrophilic molecules of less than 1 kilodalton, including adenosine triphosphate (ATP) (Bao et al. 2004; Wang et al. 2013). On several occasions, Panx1 channels have been linked to cell death (Chekeni et al. 2010; Cisneros-Mejorado et al. 2015;

Europe PMC Funders Author Manuscripts

Europe PMC Funders Author Manuscripts

Gulbransen et al. 2012; Orellana et al. 2011a; Orellana et al. 2011b; Sandilos et al. 2012; Xiao et al. 2012) and inflammatory processes (Bao et al. 2013; Csak et al. 2011; Ganz et al. 2011; Qu et al. 2011; Silverman et al. 2009). Specifically, Panx1 channels play a role in inflammatory responses by facilitating cleavage of pro-caspase1 (Casp1) in the NACHT, LRR, and pyrin domain-containing protein 3 (Nalp3) inflammasome, an intracellular multiprotein complex that activates interleukin (IL) 1β and IL-18 (Brough et al. 2009; Marina-García et al. 2008; Silverman et al. 2009). In this context, activation of the Nalp3 inflammasome and elevated hepatic Panx1 levels have been observed upon ischemia-reperfusion injury (Kim et al. 2015) as well as in experimentally induced non-alcoholic steatohepatitis in mouse (Csak et al. 2011; Ganz et al. 2011; Xiao et al. 2012). Furthermore, apoptotic cells release “find me” signals *via* Panx1 channels at the earliest stages of cell death in order to recruit phagocytes. Panx1 itself serves as a target of effector caspases 3 and 7, and a specific caspase-cleavage site within Panx1 is essential for its channel opening during apoptosis (Chekeni et al. 2010; Elliott et al. 2009). In addition, Panx1 channels have been described to orchestrate chemotaxis of neutrophils in gradient fields (Bao et al. 2013).

Given the documented involvement of Panx1 pores in inflammation and cell death, it is conceivable to assume that these channels also underlie hepatotoxicity induced by APAP. To determine whether or not this holds true, ^{10}Panx1, a well-established inhibitor of Panx1 channels (Orellana et al. 2011b; Pelegrin et al. 2008; Pelegrin and Surprenant 2006; Thompson et al. 2008), was tested in the present study for its potential to reduce liver damage caused by APAP. The outcome of Panx1 channel inhibition was evaluated based on several parameters related to liver cell death, inflammation, oxidative stress and regeneration.

2 Methods and materials

2.1 Chemicals and reagents

^{10}Panx1 (WRQAAFVDSY) was synthesized by ThermoFisher (Germany) with purity of at least 90%. All other chemicals were commercially available products of analytical grade and were supplied by Sigma (USA), unless specified otherwise.

2.2 Animals and treatment

In this study, 8-week to 10-week old male C57BL/6 mice (Jackson Laboratories, USA) were used and were housed in the animal facility of the Department of Pathology at the School of Veterinary Medicine and Animal Science of the University of São Paulo. The animals were kept in a room with ventilation (16-18 air changes/hour), relative humidity (45-65%), controlled temperature (20-24°C) and light/dark cycle 12:12, and were given water and balanced diet (NUVILAB-CR1, Nuvital Nutrientes LTDA, Brazil) *ad libitum*. In a first set of experiments, mice were starved 15-16 hours *prior* to APAP or vehicle (saline; 0.9% NaCl) administration. APAP was dissolved in saline, slightly heated and injected (30-37°C) intraperitoneally at 300 mg/kg body weight after which animals regained free access to food (Maes et al. 2016c). In other experiments, mice received APAP and after 1.5 hours were additionally administered either 10 mg/kg ^{10}Panx1 dissolved in saline or only saline through retro-orbital injection of volumes not exceeding 150 μl. The conditions for administration

Europe PMC Funders Author Manuscripts

Europe PMC Funders Author Manuscripts

of ^{10}Panx1 were optimized during preliminary testing. No overt signs of organ toxicity were observed upon gross necropsy and histopathological examination (data not shown). Mice were euthanized at the start of the experiment and 1, 3, 6, 24 and 48 hours after APAP or saline injection by exsanguination during sampling under isoflurane-induced anesthesia. Blood, collected by cardiac puncture, was drawn into a heparinized syringe and centrifuged for 10 minutes at 1503x*g*, and serum was stored at -20°C. Livers were excised and fragments were fixed in 10% phosphate-buffered formalin or snap-frozen in liquid nitrogen with storage at -80°C. This study has been approved by the Committee on Bio-ethics of the School of Veterinary Medicine and Animal Science of the University of São Paulo (protocol number 9999100314), and all animals received humane care according to the criteria outlined in the "Guide for the Care and Use of Laboratory Animals".

2.3 Gene expression analysis

Total RNA was extracted from liver tissue using a GenElute™ Mammalian Total RNA Purification Miniprep Kit and an On-Column DNase I Digestion Set according to the manufacturer's instructions. Purity and quantification of isolated RNA were measured spectrophotometrically using a Nanodrop® ND-100 Spectrophotometer (Thermo Scientific, USA). A cut-off ratio between 1.8 and 2.1 for the absorption at 260/280 nm was used for assessing purity. Then, 2 μg RNA was reversely transcribed into cDNA with an iScript™ cDNA Synthesis Kit (Bio-Rad, USA) using an iCycler iQ™ (Bio-Rad, USA) followed by cDNA purification using a GenElute™ PCR Clean-Up Kit. cDNA products were quantitatively amplified using Taqman probes and primers (Applied Biosystems, USA) targeted towards Panx1 and candidate reference genes (Table 1). All samples were analyzed in duplicate. Each run included a serial dilution of a pooled cDNA mix from all cDNA samples and 2 no template controls to estimate the quantitative polymerase chain reaction efficiency. For reverse transcription quantitative real-time polymerase chain reaction (RT-qPCR) analysis, a reaction mix was prepared containing TaqMan® Fast Advanced Master Mix (Applied Biosystems, USA), Assay-on-Demand™ Gene Expression Assay Mix (Applied Biosystems, USA) and cDNA diluted in nuclease-free water. The qPCR conditions, using a StepOnePlus™ real-time PCR system (Life Technologies, USA), included incubation for 20 seconds at 95°C followed by 40 cycles of denaturation for 1 second at 95°C and annealing for 20 seconds at 60°C. Efficiency was estimated by StepOne Plus™ system's software and only data with PCR efficiency between 90% and 110% were used. Stable candidate reference genes for normalization purposes were identified out of a pool of 6 genes as determined by geNorm using the qbase$^+$ software (Biogazelle, Belgium) (Table 1) (Vandesompele et al. 2002). The resulting ΔCq-values of the test samples were normalized to those of the calibrator samples, yielding ΔΔCq values. Relative alterations (fold change) in RNA levels were calculated according to the Livak $2^{-\Delta\Delta Cq}$ formula (Livak and Schmittgen 2001), where the average expression of untreated animals at the 0 hour time point is set to 1.

2.4 Protein expression analysis

Flash frozen liver tissue was homogenized in radio-immunoprecipitation assay buffer (Thermo Scientific, USA) containing Halt™ protease and phosphatase inhibitor cocktail (Thermo Scientific, USA), and ethylenediaminetetra-acetic acid (Thermo Scientific, USA). Following sonication for 30 seconds, samples were rotated for 15 minutes at 4°C. Cell

Europe PMC Funders Author Manuscripts

Europe PMC Funders Author Manuscripts

lysates were centrifuged at 14000x*g* for 5 minutes and protein concentrations were determined in the supernatants by means of a bicinchoninic acid assay (Pierce, USA) with bovine serum albumin as a standard. Proteins were separated on 10% Mini-Protein® TGX Stain-Free™ precast gels (Bio-Rad, USA) using electrophoresis and blotted onto polyvinylidene difluoride membranes (Bio-Rad, USA) following activation and quantification of the stain-free loading. Subsequent blocking of the membranes was performed with blocking buffer, 5% non-fatty milk in Tris-buffered saline solution (20 mM Tris and 150 mM NaCl) containing 0.1% Tween-20 (TBS/T). Membranes were incubated overnight at 4°C with primary antibody directed against Panx1 (HPA016930, Sigma, USA), diluted 1:250 in blocking buffer followed by incubation for 1 hour at room temperature with polyclonal goat anti-rabbit secondary antibody (Dako, Denmark) diluted 1:500 in blocking buffer. Excessive antibody was removed by washing the membranes several times in TBS/T. Detection of the proteins was carried out by means of a Pierce™ enhanced chemiluminescence Western blotting substrate kit (Thermo Scientific, USA) according to the manufacturer's instructions. Densitometric analysis was performed using Image Lab 5.0 software (Bio-Rad, USA). For semiquantification purposes, Panx1 signals were normalized against the total protein content and expressed as relative alterations compared to untreated animals.

2.5 Pannexin protein localization analysis

Flash frozen liver tissue samples were embedded in Tissue Freezing Medium® (Leica, UK). Then, 10 μm liver sections were fixed in acetone for 10 minutes at -20°C. Liver sections were incubated with primary antibodies directed against Panx1 (HPA016930, Sigma, USA), diluted 1:500 in blocking buffer containing phosphate-buffered saline supplemented with 0.1% NaN_3 and 1% bovine serum albumin during 1 hour at 37°C. After extensive rinsing with phosphate-buffered saline supplemented with 0.5% Tween-20, samples were incubated with polyclonal goat anti-rabbit Alexa Fluor® 488-conjugated secondary antibody (Jackson ImmunoResearch, USA), diluted 1:500 in blocking buffer. Nuclei were stained with 1 μg/ml propidium iodide and samples were mounted with Vectashield (Vector Laboratories, USA). Detection was performed by fluorescence microscopy (Nikon Eclipse T*i*, Japan) using an iterative Lucy-Richardson deconvolution algorithm.

2.6 Histopathological liver examination

For microscopic evaluation, formalin-fixed liver fragments were embedded in paraffin, and 5 μm sections were cut and stained with hematoxylin-eosin for blinded evaluation of liver damage as described elsewhere (Gujral et al. 2002). The percentage of necrosis was estimated by evaluating the number of microscopic fields with necrosis compared to the cross-sectional areas of the entire section. The histological evaluation was performed in a blinded fashion. Pictures were taken with a KF2 microscope (Carl Zeiss, USA).

2.7 Analysis of hepatic protein adducts

APAP-protein adducts were measured by high-pressure liquid chromatography with electrochemical detection as previously described (Muldrew et al. 2002) with some modifications (McGill et al. 2013). Briefly, low molecular weight compounds were removed *via* Bio-spin 6 columns (Bio-Rad, USA) and the protein fraction was subsequently digested

Europe PMC Funders Author Manuscripts

Europe PMC Funders Author Manuscripts

with proteases to liberate APAP-cysteine conjugates. The protein-derived APAP-cysteine conjugates were quantified and normalized to protein concentration in the original samples.

2.8 Analysis of serum aminotransaminases

Alanine aminotransferase (ALT) and aspartate aminotransferase (AST) levels were measured with an automated spectrophotometric Labmax 240 analyzer (Labtest Diagnostica, Brazil) after appropriate dilution of the collected serum samples. Values were expressed in IU/L.

2.9 Analysis of liver and serum cytokines

Liver tissue was homogenized in Complete Lysis-M buffer with protease inhibitors (Roche, Germany). Homogenates were centrifuged at 14000x*g* for 15 minutes at 4°C and protein concentrations in supernatants were determined according to the Bradford procedure (Bradford 1976) using a commercial kit (Bio-Rad, USA) with bovine serum albumin as a standard. Enzyme-linked immunosorbent assay (ELISA) kits were used to measure levels of mouse interleukin IL-1β, IL-6, IL-10, interferon (IFN)γ, tumor necrosis factor (TNF)α (BD Biosciences, USA) and IL-18 (Medical and Biological Laboratories, Japan) as previously described (Maes et al. 2016a; Maes et al. 2016b).

2.10 Hepatic leukocyte recruitment analysis

For these experiments, 8-week old male C57BL/6 mice were obtained from Janvier (France). The animals were housed at the Lab of Cellular and Molecular Immunology of the Vrije Universiteit Brussel. Mice were starved 15 hours *prior* to intraperitoneal administration of APAP at 300 mg/kg body weight after which animals regained free access to food. Mice were euthanized 24 hours after APAP injection by carbon dioxide. Livers were collected after perfusion with phosphate-buffered saline, chopped finely and incubated for 20 minutes with 1 mg/ml collagenase A and 10 IU/ml DNase (Roche, Germany) in a shaking water bath at 37°C. After filtration through a 70 μm filter, cells were centrifuged at 400x*g* and 4°C for 5 minutes. Red blood cells were lyzed with 8.3 g/l NH_4Cl in 10 mM Tris-buffer. To check leukocyte recruitment, 10^6 cells were stained with allophycocyanin cyanine 7-labeled pan anti-cluster of differentiation (CD) 45 antibody (BioLegend, USA), fluorescein isothiocyanate labeled Ly6G antibody, phycoerythrin cyanine 7-labeled CD11b antibody, peridinin chlorophyll cyanine 5.5-labeled streptavidine antibody, biotin labeled F4/80 antibody and brilliant violet 421-labeled Ly6C antibody at 4°C for 20 minutes. Subsequently, cell suspensions were subjected to flow cytometry. For intracellular TNFα determination, 10^6 cells were incubated during 4 hours at 37°C with BD GolgiPlug™ (BD Biosciences, USA) following the manufacturer's instructions. Thereafter, cells were incubated with the antibodies mentioned above, used to check the leukocyte recruitment, for 20 minutes at 4°C. Cells were then fixed and permeabilized with Cytofix/Cytoperm™ (BD Biosciences, USA) following the manufacturer's instructions. Fixed cells were stained with phycoerythrin-labeled anti-TNFα (BD Biosciences, USA) or IgG1 isotype antibodies for 20 minutes at 4°C. Next, cell suspensions were subjected to flow cytometry. The results were analyzed with a FACScantoll (BD Biosciences, USA) and FlowJo software (TreeStar, USA). All experiments were carried out in accordance with the guidelines provided by the ethical committee on animal experimentation of the Vrije Universiteit Brussel.

Europe PMC Funders Author Manuscripts

Europe PMC Funders Author Manuscripts

2.11 Hepatic glutathione and glutathione disulfide analysis

GSH and glutathione disulfide (GSSG) levels in liver tissue were measured using a modified Tietze assay (Jaeschke and Mitchell 1990). Briefly, frozen liver tissue was homogenized in 3% sulfosalicylic acid/ethylendiaminetetra-acetic acid and centrifuged at 18000x*g* for 5 minutes at 4°C to remove precipitated proteins. After further dilution with potassium phosphate buffer, samples were assayed with a cycling reaction utilizing GSH reductase and dithionitrobenzoic acid. Measurement of GSSG was performed using the same method after trapping GSH with *N*-ethylmaleimide and removal by solid phase extraction (Jaeschke and Mitchell 1990). GSSG content was expressed as GSH equivalents.

2.12 Proliferating cell nuclear antigen protein analysis

Protein expression of proliferating cell nuclear antigen (PCNA) was studied by means of immunoblotting as previously described (Bajt et al. 2000; Maes et al. 2016b). In essence, liver tissue protein lysates (50 μg *per* lane) were resolved on 4-20% sodium dodecyl sulphate polyacrylamide gel electrophoresis under reducing conditions. Separated proteins were transferred to polyvinylidene difluoride membranes (Millipore Corporation, USA) and blocked overnight at 4°C with 5% milk in TBS/T. After washing with TBS/T, membranes were incubated with a mouse monoclonal anti-PCNA antibody (Santa Cruz Biotechnology, USA), diluted 1/2000 in blocking buffer for 2 hours at room temperature. Membranes were washed and incubated with appropriate secondary horseradish peroxidase-coupled antibody (Santa Cruz Biotechnology, USA) for 1 hour at room temperature. Proteins were visualized by enhanced chemiluminescence (Amersham Biosciences, USA) according to the manufacturer's instructions. Densitometric analysis was performed with a GS170 Calibrated Imaging Densitometer (Bio-Rad, USA) using Quantity One 4.0.3. software (Bio-Rad, USA). For semiquantification purposes, PCNA signals were normalized against β-actin signals.

2.13 Statistical analysis

All data were expressed as mean ± standard error of the mean (SEM). Results were statistically processed by 1-way analysis of variance (ANOVA) followed by *post hoc* Bonferroni tests or 2-tailed unpaired student *t*-tests and Welch's correction using GraphPad Prism6 software, with probability (*p*) values of less than or equal to 0.05 considered as significant.

3 Results

3.1 APAP overdosing induces hepatic mRNA and protein expression of Panx1

In order to show the involvement of Panx1 channels in APAP-induced hepatotoxicity, Panx1 RNA and protein levels were measured by RT-qPCR analysis and immunoblot analysis, respectively, at different time points after APAP or vehicle administration. This revealed significantly enhanced Panx1 gene transcription and protein levels in liver tissue after 6 hours ($p < 0.05$), steeply increasing towards 24 hours following APAP treatment ($p < 0.001$ for RNA level and $p < 0.0001$ for protein level) compared to the vehicle control (Fig. 1a,b). Similar changes were seen in gene transcription of the Nalp3 inflammasome components Nalp3, Casp1 and apoptosis-associated speck-like protein containing a C-terminal caspase-

Europe PMC Funders Author Manuscripts

Europe PMC Funders Author Manuscripts

recruitment domain (ASC) (Supplementary Fig. 1). During immunoblot analysis, Panx1 was detected as 3 signals, representing the non-glycosylated core (Gly0), the high-mannose (Gly1) and the complex glycosylated species (Gly2) (Fig. 1b) (Boassa et al. 2007; Penuela et al. 2009). In control mice, Panx1 was mainly found in the Gly0 (49.5% ± 1.4) and Gly2 (36.6% ± 3.3) status. However, 6 hours and 24 hours after APAP administration, a transition to the Gly2 species was detected, namely 84.5% ± 6.6 and 90.5% ± 1.9, respectively (Table 2). Previous studies suggested that *N*-glycosylation of Panx1 might play a key role in regulating its traffic to the cell surface (Boassa et al. 2007). Indeed, the Gly2 species is more abundant at the cell plasma membrane, while both the Gly0 and Gly1 variants are preferentially found as residents of the endoplasmic reticulum (Penuela et al. 2009). In addition, increased levels of Gly2 in mouse brain were reported after experimental induction of hippocampal seizures by cobalt treatment (Mylvaganam et al. 2010). Nevertheless, immunohistochemistry analysis showed the presence of Panx1 both intracellularly and at the cell plasma membrane 6 hours and 24 hours after APAP overdosing compared to the sole plasma membrane localization in the control animals (Fig. 2a,b). Part of the intracellular Panx1 population was identified in the nuclear compartment after APAP overdosing using Lucy-Richardson deconvolution algorithm. In addition, Panx1 was evenly distributed over the liver acinar region in naive and saline-treated animals, as similar signals were found in the periportal and pericentral zones (Fig. 2a). However, 6 and 24 hours after APAP overdosing, altered expression was found in the pericentral zones (Fig. 2a).

3.2 Panx1 channel inhibition diminishes liver cell damage following APAP overdosing

APAP is well known to cause hepatic cell death in a zonated pattern. Specifically, necrotic patches appear around the central vein, where expression of cytochrome P450 enzymes responsible for NAPQI formation is the highest (Lee et al. 1996). In the current study, these necrotic areas were clearly detectable microscopically 24 hours after administration of APAP. There was a modest trend towards less necrosis upon Panx1 inhibition, although not significant (Fig. 3a). In order to verify whether the morphological findings are reflected at the clinical chemistry level, serum amounts of ALT and AST were measured in APAP-overdosed mice whether or not treated with ^{10}Panx1. In all animals tested in this study, ALT and AST serum levels were elevated, progressively increasing towards 6 hours and 24 hours. Most importantly, significantly reduced serum levels of ALT ($p < 0.001$) and AST ($p < 0.0001$) were found after 24 hours in the ^{10}Panx1-treated mice (Fig. 3b).

3.3 Panx1 channel inhibition does not affect hepatic protein adduct formation following APAP overdosing

The mechanism of toxicity of APAP, and thus the mouse model as such, depends on the formation of the deleterious reactive metabolite NAPQI. In case of APAP overdosing, NAPQI reacts with protein sulfhydryl groups, which leads to the formation of noxious liver protein adducts (Mitchell et al. 1973). To confirm that the diminished liver damage after treatment with ^{10}Panx1 occurs independently of NAPQI formation, APAP-protein adducts were measured 3 hours and 6 hours after APAP administration. The APAP-protein adducts were detectable in all mice, yet no differences were observed between the different experimental groups (Fig. 4).

Europe PMC Funders Author Manuscripts

Europe PMC Funders Author Manuscripts

3.4 Panx1 channel inhibition differentially affects serum and liver cytokine levels following APAP overdosing

Panx1 channels have been identified as major drivers of inflammatory responses (Brough et al. 2009; Ganz et al. 2011; Kim et al. 2015; Marina-García et al. 2008; Silverman et al. 2009). For this reason, a number of cytokines, namely IL-1β, IL-6, IL-10, IL-18, IFNγ and TNFα, which are considered of relevance for controlling hepatic injury-associated inflammation (Blazka et al. 1995; Cover et al. 2006; Ishida et al. 2002; James et al. 2005; Lawson et al. 2000), were evaluated 24 hours after APAP administration. Serum levels of these cytokines are reflective of the severity of liver injury, though they may not be consistent with corresponding hepatic levels *per se*. Therefore, IL-1β, IL-6, IL-10, IL-18, IFNγ and TNFα were also measured by ELISA analysis in liver homogenates obtained from APAP-overdosed mice whether or not treated with ^{10}Panx1 (Fig. 5). Administration of ^{10}Panx1 to APAP-overdosed animals reduced overall inflammation as evidenced by significantly lower ($p < 0.05$, $p < 0.01$ or $p < 0.001$) liver levels of IL-1β, IL-6, IL-10, IFNγ and TNFα compared to vehicle-treated mice. For IL-6, IL-10 and TNFα, this was parallelled in serum. IFNγ serum levels were below the detection limit for both experimental groups (data not shown). Rather surprisingly, IL-18 serum quantities were not affected by ^{10}Panx1 and were significantly increased ($p < 0.05$) in liver (Fig. 5).

3.5 Panx1 channel inhibition reduces recruitment of neutrophils following APAP overdosing

During hepatocyte cell death, a number of molecules, so-called damage-associated molecular patterns, are released, which can activate macrophages and induce cytokine formation (Antoine et al. 2009; Martin-Murphy et al. 2010). These inflammatory mediators trigger neutrophils and monocytes leading to the recruitment of these leukocytes to the liver. Monocyte migration has been reported to be mediated in part by Panx1-dependent extracellular ATP release *in vitro* (Xiao et al. 2012) and finetuned chemotactic responses of neutrophils seem to require Panx1 signaling (Bao et al. 2013). To check if this also holds true *in vivo*, *in casu* in a model of APAP-induced hepatotoxicity, leukocyte recruitment into the liver of APAP-overdosed animals whether or not treated with ^{10}Panx1 was evaluated 24 hours after APAP administration using flow cytometry analysis. Living non-doublet cells were first selected by forward and side scatter, out of which all $CD45^+$ non-parenchymal cells were included. From this, neutrophils were detected as $CD45^+CD11b^{hi}Ly6G^+$ cells, while Kupffer cells were detected as $CD45^+Ly6G^-F4/80^{hi}CD11b^{int}$ cells. The inflammatory monocyte population was selected as $CD45^+CD11b^{hi}Ly6C^{hi}F4/80^{lo}$ cells (Fig. 6a). Compared to untreated animals, APAP-overdosed mice showed a lower amount of Kupffer cells ($p < 0.0001$), but increased liver levels of neutrophils and inflammatory monocytes ($p < 0.0001$) (Fig. 6b). However, when Panx1 channels were blocked, a significantly reduced ($p < 0.0001$) amount of neutrophils was recruited into the liver (Fig. 6b). As neutrophils produce TNFα, this could possibly explain the lowered liver levels of this pro-inflammatory cytokine in ^{10}Panx1-treated animals (Fig. 5). However, the reduced amount of TNFα can not only be attributed to reduction in TNFα-producing neutrophils, but also to reduced ($p < 0.05$) production by inflammatory monocytes when Panx1 channels are inhibited (Fig. 6c).

Europe PMC Funders Author Manuscripts

Europe PMC Funders Author Manuscripts

3.6 Panx1 channel inhibition alters the liver oxidative status following APAP overdosing

In healthy cells, more than 99% of the total glutathione pool occurs in the reduced form (GSH) and less than 1% exists in the oxidized form (GSSG) (Jaeschke and Mitchell 1990). An increased GSSG/GSH ratio is considered indicative of oxidative stress, as is the case for APAP-induced liver injury, which is inherently accompanied by GSH depletion (Jaeschke 1990; Knight et al. 2001). In the present study, the GSH levels of all animals were depleted 3 hours after APAP administration with a gradual recovery after 6 and 24 hours (Fig. 7a). Nonetheless, neither hepatic GSSG levels (Fig. 7b) nor the GSSG/GSH ratio (Fig. 7c) were significantly altered by ^{10}Panx1 in APAP-overdosed mice. However, inhibition of Panx1 channels significantly ($p < 0.001$) upregulated GSH amounts in liver 24 hours following APAP overdosing (Fig. 7a). The relevance of this finding is unclear. ^{10}Panx1 may enhance GSH resynthesis, which could be indicative of the improved tissue viability. Alternatively, the higher GSH levels could contribute to its protective effect by improving scavenging of reactive oxygen species.

3.7 Panx1 channel inhibition promotes liver regeneration following APAP overdosing

The liver has a considerable regenerative capacity. In addition to injury mechanisms, initiation of regeneration is critical for repair of damaged liver tissue and recovery after APAP-induced liver injury (Mehendale 2005). Dividing hepatocytes adjacent to necrotic areas replace dead counterparts (Bajt et al. 2003). Cycling cells typically display high production of PCNA, an auxiliary protein to DNA polymerase that is essential for both DNA synthesis and repair. Consequently, PCNA expression is commonly used as a parameter to monitor regenerative activity in liver following injury (Bajt et al. 2003). In the present study, hepatic protein levels of PCNA, assessed by immunoblot analysis, were significantly higher ($p < 0.05$) in APAP-overdosed mice treated with ^{10}Panx1 compared to solely APAP-overdosed animals after 24 hours (Fig. 8), while no significant difference was found after 48 hours (data not shown). This points to early stimulation of regeneration upon Panx1 channel inhibition following APAP overdosing, which might reflect the reduced injury in these animals.

4 Discussion

Pannexins were first described in 2000 and form hexameric plasma membrane channels that support paracrine signaling (Panchin et al. 2000; Penuela et al. 2013; Wang et al. 2013). Only in the last few years, a handful of studies have addressed pannexins in liver, whereby Panx1 was detected in hepatocytes (Bruzzone et al. 2003; Csak et al. 2011; Ganz et al. 2011; Kim et al. 2015; Xiao et al. 2012) and Kupffer cells (Sáez et al. 2014). A number of biochemical messengers are known to be released in the extracellular milieu through pannexin channels with the most extensively studied one being ATP (Penuela et al. 2013; Wang et al. 2013). By doing so, these channels fulfill physiological functions, in particular in cellular differentiation, as shown in keratinocytes (Celetti et al. 2010), neurons (Swayne et al. 2010) and chondrocytes (Iwamoto et al. 2010). Pannexin channels equally play pathological roles, specifically by facilitating inflammation (Brough et al. 2009; Marina-García et al. 2008; Silverman et al. 2009) and cell death (Chekeni et al. 2010; Elliott et al. 2009). In this respect, Panx1 channels were found to contribute to experimentally induced

Europe PMC Funders Author Manuscripts

Europe PMC Funders Author Manuscripts

lipo-apoptosis in hepatocytes (Xiao et al. 2012). In the present study, it was investigated whether these channels are also involved in APAP-mediated acute hepatotoxicity. It was found that liver expression of Panx1 is strongly upregulated upon APAP overdosing at the transcriptional and translational level. In addition, the glycosylation status of the hepatic Panx1 was altered after APAP-induced hepatotoxicity in mice. In particular, a transition from the non-glycosylated Gly0 variant to the complex glycosylated Gly2 species was detected. Glycosylation of Panx1 has been described to be a prerequisite for channel insertion into the plasma membrane (Boassa et al. 2007; Mylvaganam et al. 2010; Penuela et al. 2009). Thus, our results may point to possible increased Panx1 channel activity in APAP-induced hepatotoxicity, although given the known issues with pannexin antibodies in this particular research field, these results should be considered with caution. In order to demonstrate an active role for these channels in APAP-triggered liver toxicity, the well-known Panx1 channel inhibitor ^{10}Panx1 was used. ^{10}Panx1 is a short peptide that mimics a sequence in the first extracellular loop moiety of Panx1 and that blocks its channel function (Pelegrin and Surprenant 2006). ^{10}Panx1 was found to act in an anti-inflammatory way and to protect against cell death in several cell types (Orellana et al. 2011b; Pelegrin et al. 2008). In the current study, ^{10}Panx1 was systemically injected 1.5 hours after APAP administration, which is the timeframe necessary for completion of APAP biotransformation and hence for formation of the deleterious NAPQI metabolite. Since the maximum depletion of GSH occurs 0.5 hours after APAP administration (McGill et al. 2013), there was no difference in GSH depletion between the study groups. In addition, no effect of ^{10}Panx1 on APAP-protein adducts was observed, suggesting that the delayed administration of ^{10}Panx1 did not have a relevant impact on reactive metabolite formation and thus not on the initial events of APAP-induced hepatotoxicity. By relying on this rationalized experimental set-up, ^{10}Panx1 was shown to reduce biochemical (serum ALT and AST levels) hallmarks of APAP-induced cell death 24 hours after APAP administration, demonstrating that Panx1 channel inhibition alleviates APAP-induced hepatotoxicity. Of note, ^{10}Panx1 did not alter Panx1 protein content nor did it affect its glycosylation status (Supplementary Fig. 2).

On several occasions, Panx1 channels have been linked to Nalp3 inflammasome activation, resulting in the extracellular release of IL-1β and IL-18, which are thought to mediate inflammatory reactions (Imaeda et al. 2009; Martinon et al. 2002). Although ^{10}Panx1 decreased liver amounts of IL-1β, no differences were detected in the serum levels of this pro-inflammatory cytokine. Furthermore, increased hepatic levels of IL-18 were found in ^{10}Panx1-treated mice. This differential outcome suggests that the beneficial effects of Panx1 channel inhibition, at least for APAP-induced hepatotoxicity, might not be related to the activation of the Nalp3 inflammasome. This was supported by the observations that ^{10}Panx1 treatment did not alter RNA expression of Nalp3 inflammasome building stones (Supplementary Fig. 3) nor did it affect Casp1 activation after APAP overdosing (data not shown). These results are in line with a previously published report demonstrating that the Nalp3 inflammasome does not appear to be a critical factor in murine APAP-induced liver injury (Williams et al. 2011). In the latter study, a similar extent of neutrophil recruitment, cytokine levels and liver injury in mice deficient for each component of the Nalp3 inflammasome (ASC, Casp1 and Nalp3) compared to wild-type animals were found. Besides IL-1β and IL-18 levels, ^{10}Panx1 administration decreased liver and serum quantities

Europe PMC Funders Author Manuscripts

Europe PMC Funders Author Manuscripts

of the pro-inflammatory cytokines IL-6, TNFα and IFNγ in APAP-overdosed mice. These findings suggest that Panx1 channel inhibition suppresses APAP-induced inflammation, yet it should be mentioned that ^{10}Panx1 equally lowered hepatic and serum amounts of IL-10, a prominent anti-inflammatory cytokine. This might be a consequence of overall lower inflammatory cytokine levels. Hepatocyte cell death and cytokine formation ultimately lead to activation and infiltration of neutrophils and monocytes in the liver. In this study, reduced infiltration of neutrophils upon treatment of APAP-overdosed mice with ^{10}Panx1 was noticed. The decreased amount of TNFα could be attributed to reduction in TNFα-producing neutrophils as well as to decreased TNFα production by inflammatory monocytes upon Panx1 channel inhibition. The contribution of neutrophils to APAP-induced injury remains controversial (Jaeschke et al. 2012). A substantial number of studies found no involvement of neutrophils in the pathophysiology of APAP-induced liver injury (Connolly et al. 2011; Cover et al. 2006; Lawson et al. 2000; Williams et al. 2010a; Williams et al. 2014; Williams et al. 2010b). Although several studies suggested a contribution of neutrophils to the late-stage injury process (Ishida et al. 2006; Liu et al. 2006; Marques et al. 2012), these reports were criticized for the same off-target effect of the neutropenia intervention used (Jaeschke et al. 2012). From the present study, it is not possible to assess whether reduced neutrophil infiltration was a cause or a consequence of ^{10}Panx1-mediated milder liver injury, yet given the extensive evidence against a direct role of neutrophils in the injury process, the attenuated inflammatory response is most likely a reflection of reduced injury in the ^{10}Panx1-treated animals. However, a direct effect of the inhibitor on neutrophils cannot be excluded, as it has been previously described that activation of neutrophils requires Panx1 signaling (Bao et al. 2013). Furthermore, increased recovery after initial depletion of the hepatic GSH levels was detected 24 hours after APAP administration in the ^{10}Panx1-treated animals. This could possibly account for the overall reduced cell death and inflammation observed in APAP-overdosed animals upon treatment with ^{10}Panx1. Indeed, GSH detoxifies NAPQI and reactive oxygen species, thereby reducing cell stress and damage. In addition, inhibition of Panx1 channels promoted regenerative activity and thus repair following APAP-induced hepatocellular injury as shown by elevated PCNA protein production.

In conclusion, the results of this study demonstrate for the first time that Panx1 channels are major actors in APAP-induced liver damage. These observations also suggest that pharmacological inhibition of these channels might be a potentially new approach, complementary to *N*-acetylcysteine treatment, in the clinical therapy of acute drug-induced hepatotoxicity.

Supplementary Material

Refer to Web version on PubMed Central for supplementary material.

Acknowledgements

This work was financially supported by the grants of the Agency for Innovation by Science and Technology in Flanders (IWT grant 131003), the European Research Council (ERC Starting Grant 335476), the Fund for Scientific Research-Flanders (FWO grants G009514N and G010214N), the University Hospital of the Vrije Universiteit Brussel-Belgium (“Willy Gepts Fonds” UZ-VUB), the University of São Paulo-Brazil, the Foundation for Research Support of the State of São Paulo (FAPESP SPEC grant 2013/50420-6) and the National Institutes of

Health (NIH grants DK102142 and P20 GM103549). The authors wish to thank Miss Tineke Vanhalewyn, Miss Dinja De Win, Miss Shirlei Meire da Silva, Miss Cintia Maria Monteiro de Araújo, Dr. André G. Oliveira, Dr. Pedro E. Marques, Dr. Gustavo B. Menezes, Mister José Alexandre Coelho Pimental and Mister Paul Claes for their dedicated technical assistance.

List of abbreviations

ALT	alanine aminotransferase
ANOVA	analysis of variance
APAP	acetaminophen
ASC	apoptosis-associated speck-like protein containing a C-terminal caspase-recruitment domain
AST	aspartate aminotransferase
ATP	adenosine triphosphate
Casp1	caspase1
CD	cluster of differentiation
ELISA	enzyme-linked immunosorbent assay
Gly	glycosylated
GSH	glutathione
GSSG	glutathione disulfide
IFNγ	interferon γ
IL-1β/6/10/18	interleukin 1β/6/10/18
n	number of repeats
Nalp3	NACHT, LRR, and pyrin domain-containing protein 3
NAPQI	*N*-acetyl-*p*-benzoquinone imine
p	probability
Panx	pannexin
PCNA	proliferating cell nuclear antigen
RT-qPCR	reverse transcription quantitative real-time polymerase chain reaction
SEM	standard error of the mean
TBS/T	Tris-buffered saline solution containing 0.1% Tween-20
TNFα	tumor necrosis factor α

Europe PMC Funders Author Manuscripts
Europe PMC Funders Author Manuscripts

Europe PMC Funders Author Manuscripts

Europe PMC Funders Author Manuscripts

References

Antoine DJ, et al. High-mobility group box-1 protein and keratin-18, circulating serum proteins informative of acetaminophen-induced necrosis and apoptosis in vivo. Toxicol Sci. 2009; 112:521–531. [PubMed: 19783637]

Bajt ML, Knight TR, Farhood A, Jaeschke H. Scavenging peroxynitrite with glutathione promotes regeneration and enhances survival during acetaminophen-induced liver injury in mice. J Pharmacol Exp Ther. 2003; 307:67–73. [PubMed: 12954812]

Bajt ML, Lawson JA, Vonderfecht SL, Gujral JS, Jaeschke H. Protection against Fas receptor-mediated apoptosis in hepatocytes and nonparenchymal cells by a caspase-8 inhibitor in vivo: evidence for a postmitochondrial processing of caspase-8. Toxicol Sci. 2000; 58:109–117. [PubMed: 11053547]

Bao L, Locovei S, Dahl G. Pannexin membrane channels are mechanosensitive conduits for ATP. FEBS Lett. 2004; 572:65–68. [PubMed: 15304325]

Bao Y, Chen Y, Ledderose C, Li L, Junger WG. Pannexin 1 channels link chemoattractant receptor signaling to local excitation and global inhibition responses at the front and back of polarized neutrophils. J Biol Chem. 2013; 288:22650–22657. [PubMed: 23798685]

Blazka ME, Wilmer JL, Holladay SD, Wilson RE, Luster MI. Role of proinflammatory cytokines in acetaminophen hepatotoxicity. Toxicol Appl Pharmacol. 1995; 133:43–52. [PubMed: 7597709]

Boassa D, Ambrosi C, Qiu F, Dahl G, Gaietta G, Sosinsky G. Pannexin1 channels contain a glycosylation site that targets the hexamer to the plasma membrane. J Biol Chem. 2007; 282:31733–31743. [PubMed: 17715132]

Bradford MM. A rapid and sensitive method for the quantitation of microgram quantities of protein utilizing the principle of protein-dye binding. Anal Biochem. 1976; 72:248–254. [PubMed: 942051]

Brough D, Pelegrin P, Rothwell NJ. Pannexin-1-dependent caspase-1 activation and secretion of IL-1beta is regulated by zinc. Eur J Immunol. 2009; 39:352–358. [PubMed: 19130485]

Bruzzone R, Hormuzdi SG, Barbe MT, Herb A, Monyer H. Pannexins, a family of gap junction proteins expressed in brain. Proc Natl Acad Sci U S A. 2003; 100:13644–13649. [PubMed: 14597722]

Celetti SJ, Cowan KN, Penuela S, Shao Q, Churko J, Laird DW. Implications of pannexin 1 and pannexin 3 for keratinocyte differentiation. J Cell Sci. 2010; 123:1363–1372. [PubMed: 20332104]

Chekeni FB, et al. Pannexin 1 channels mediate 'find-me' signal release and membrane permeability during apoptosis; Nature. 2010; 467:863–867. [PubMed: 20944749]

Cisneros-Mejorado A, et al. Blockade of P2X7 receptors or pannexin-1 channels similarly attenuates postischemic damage. J Cereb Blood Flow Metab. 2015; 35:843–850. [PubMed: 25605289]

Connolly MK, et al. Dendritic cell depletion exacerbates acetaminophen hepatotoxicity. Hepatology. 2011; 54:959–968. [PubMed: 21574173]

Cover C, Liu J, Farhood A, Malle E, Waalkes MP, Bajt ML, Jaeschke H. Pathophysiological role of the acute inflammatory response during acetaminophen hepatotoxicity. Toxicol Appl Pharmacol. 2006; 216:98–107. [PubMed: 16781746]

Csak T, Ganz M, Pespisa J, Kodys K, Dolganiuc A, Szabo G. Fatty acid and endotoxin activate inflammasomes in mouse hepatocytes that release danger signals to stimulate immune cells. Hepatology. 2011; 54:133–144. [PubMed: 21488066]

Dahlin DC, Miwa GT, Lu AY, Nelson SD. N-acetyl-p-benzoquinone imine: a cytochrome P-450-mediated oxidation product of acetaminophen; Proc Natl Acad Sci U S A. 1984; 81:1327–1331. [PubMed: 6424115]

Elliott MR, et al. Nucleotides released by apoptotic cells act as a find-me signal to promote phagocytic clearance. Nature. 2009; 461:282–286. [PubMed: 19741708]

Ganz M, Csak T, Nath B, Szabo G. Lipopolysaccharide induces and activates the Nalp3 inflammasome in the liver. World J Gastroenterol. 2011; 17:4772–4778. [PubMed: 22147977]

Gujral JS, Knight TR, Farhood A, Bajt ML, Jaeschke H. Mode of cell death after acetaminophen overdose in mice: apoptosis or oncotic necrosis? Toxicol Sci. 2002; 67:322–328. [PubMed: 12011492]

Europe PMC Funders Author Manuscripts

Europe PMC Funders Author Manuscripts

Gulbransen BD, et al. Activation of neuronal P2X7 receptor-pannexin-1 mediates death of enteric neurons during colitis. Nat Med. 2012; 18:600–604. [PubMed: 22426419]

Ichai P, Samuel D. Epidemiology of liver failure. Clin Res Hepatol Gastroenterol. 2011; 35:610–617. [PubMed: 21550329]

Imaeda AB, et al. Acetaminophen-induced hepatotoxicity in mice is dependent on Tlr9 and the Nalp3 inflammasome. J Clin Invest. 2009; 119:305–314. [PubMed: 19164858]

Ishida Y, Kondo T, Kimura A, Tsuneyama K, Takayasu T, Mukaida N. Opposite roles of neutrophils and macrophages in the pathogenesis of acetaminophen-induced acute liver injury. Eur J Immunol. 2006; 36:1028–1038. [PubMed: 16552707]

Ishida Y, Kondo T, Ohshima T, Fujiwara H, Iwakura Y, Mukaida N. A pivotal involvement of IFN-gamma in the pathogenesis of acetaminophen-induced acute liver injury. FASEB J. 2002; 16:1227–1236. [PubMed: 12153990]

Iwamoto T, Nakamura T, Doyle A, Ishikawa M, de Vega S, Fukumoto S, Yamada Y. Pannexin 3 regulates intracellular ATP/cAMP levels and promotes chondrocyte differentiation. J Biol Chem. 2010; 285:18948–18958. [PubMed: 20404334]

Jaeschke H. Glutathione disulfide formation and oxidant stress during acetaminophen-induced hepatotoxicity in mice in vivo: the protective effect of allopurinol. J Pharmacol Exp Ther. 1990; 255:935–941. [PubMed: 2262912]

Jaeschke H, Mitchell JR. Use of isolated perfused organs in hypoxia and ischemia/reperfusion oxidant stress. Methods Enzymol. 1990; 186:752–759. [PubMed: 2233332]

Jaeschke H, Williams CD, Ramachandran A, Bajt ML. Acetaminophen hepatotoxicity and repair: the role of sterile inflammation and innate immunity; Liver Int. 2012; 32:8–20. [PubMed: 21745276]

James LP, Kurten RC, Lamps LW, McCullough S, Hinson JA. Tumour necrosis factor receptor 1 and hepatocyte regeneration in acetaminophen toxicity: a kinetic study of proliferating cell nuclear antigen and cytokine expression. Basic Clin Pharmacol Toxicol. 2005; 97:8–14. [PubMed: 15943753]

Jollow DJ, Mitchell JR, Potter WZ, Davis DC, Gillette JR, Brodie BB. Acetaminophen-induced hepatic necrosis. II. Role of covalent binding in vivo. J Pharmacol Exp Ther. 1973; 187:195–202. [PubMed: 4746327]

Kim HY, Kim SJ, Lee SM. Activation of NLRP3 and AIM2 inflammasomes in Kupffer cells in hepatic ischemia/reperfusion. Febs J. 2015; 282:259–270. [PubMed: 25327779]

Knight TR, Kurtz A, Bajt ML, Hinson JA, Jaeschke H. Vascular and hepatocellular peroxynitrite formation during acetaminophen toxicity: role of mitochondrial oxidant stress. Toxicol Sci. 2001; 62:212–220. [PubMed: 11452133]

Lawson JA, Farhood A, Hopper RD, Bajt ML, Jaeschke H. The hepatic inflammatory response after acetaminophen overdose: role of neutrophils. Toxicol Sci. 2000; 54:509–516. [PubMed: 10774834]

Le Vasseur M, Lelowski J, Bechberger JF, Sin WC, Naus CC. Pannexin 2 protein expression is not restricted to the CNS. Front Cell Neurosci. 2014; 8:392. [PubMed: 25505382]

Lee SS, Buters JT, Pineau T, Fernandez-Salguero P, Gonzalez FJ. Role of CYP2E1 in the hepatotoxicity of acetaminophen. J Biol Chem. 1996; 271:12063–12067. [PubMed: 8662637]

Lee WM. Etiologies of acute liver failure. Semin Liver Dis. 2008; 28:142–152. [PubMed: 18452114]

Liu ZX, Han D, Gunawan B, Kaplowitz N. Neutrophil depletion protects against murine acetaminophen hepatotoxicity. Hepatology. 2006; 43:1220–1230. [PubMed: 16729305]

Livak KJ, Schmittgen TD. Analysis of relative gene expression data using real-time quantitative PCR and the $2^{-\Delta\Delta C}$ method. Methods. 2001; 25:402–408. [PubMed: 11846609]

Maes M, et al. Involvement of connexin43 in acetaminophen-induced liver injury. Biochim Biophys Acta. 2016a; 1862:1111–1121. [PubMed: 26912412]

Maes M, et al. Connexin32: a mediator of acetaminophen-induced liver injury? Toxicol Mech Methods. 2016b; 26:88–96. [PubMed: 26739117]

Maes M, Vinken M, Jaeschke H. Experimental models of hepatotoxicity related to acute liver failure. Toxicol Appl Pharmacol. 2016c; 290:86–97. [PubMed: 26631581]

Europe PMC Funders Author Manuscripts

Marina-García N, Franchi L, Kim YG, Miller D, McDonald C, Boons GJ, Núñez G. Pannexin-1-mediated intracellular delivery of muramyl dipeptide induces caspase-1 activation via cryopyrin/NLRP3 independently of Nod2. J Immunol. 2008; 180:4050–4057. [PubMed: 18322214]

Marques PE, et al. Chemokines and mitochondrial products activate neutrophils to amplify organ injury during mouse acute liver failure. Hepatology. 2012; 56:1971–1982. [PubMed: 22532075]

Martin-Murphy BV, Holt MP, Ju C. The role of damage associated molecular pattern molecules in acetaminophen-induced liver injury in mice. Toxicol Lett. 2010; 192:387–394. [PubMed: 19931603]

Martinon F, Burns K, Tschopp J. The inflammasome: a molecular platform triggering activation of inflammatory caspases and processing of proIL-beta. Mol Cell. 2002; 10:417–426. [PubMed: 12191486]

McGill MR, et al. Plasma and liver acetaminophen-protein adduct levels in mice after acetaminophen treatment: Dose-response, mechanisms, and clinical implications. Toxicol Appl Pharmacol. 2013; 269:240–249. [PubMed: 23571099]

Mehendale HM. Tissue repair: an important determinant of final outcome of toxicant-induced injury. Toxicol Pathol. 2005; 33:41–51. [PubMed: 15805055]

Mitchell JR, Jollow DJ, Potter WZ, Davis DC, Gillette JR, Brodie BB. Acetaminophen-induced hepatic necrosis. I. Role of drug metabolism. J Pharmacol Exp Ther. 1973; 187:185–194. [PubMed: 4746326]

Muldrew KL, James LP, Coop L, McCullough SS, Hendrickson HP, Hinson JA, Mayeux PR. Determination of acetaminophen-protein adducts in mouse liver and serum and human serum after hepatotoxic doses of acetaminophen using high-performance liquid chromatography with electrochemical detection. Drug Metabol Dispos. 2002; 30:446–451.

Mylvaganam S, et al. Hippocampal seizures alter the expression of the pannexin and connexin transcriptome. J Neurochem. 2010; 112:92–102. [PubMed: 19840216]

Orellana JA, et al. ATP and glutamate released via astroglial connexin 43 hemichannels mediate neuronal death through activation of pannexin 1 hemichannels. J Neurochem. 2011a; 118:826–840. [PubMed: 21294731]

Orellana JA. Amyloid beta-induced death in neurons involves glial and neuronal hemichannels. J Neurosci. 2011b; 31:4962–4977. [PubMed: 21451035]

Panchin Y, Kelmanson I, Matz M, Lukyanov K, Usman N, Lukyanov S. A ubiquitous family of putative gap junction molecules. Curr Biol. 2000; 10:473–474.

Pelegrin P, Barroso-Gutierrez C, Surprenant A. P2X7 receptor differentially couples to distinct release pathways for IL-1beta in mouse macrophage; J Immunol. 2008; 180:7147–7157. [PubMed: 18490713]

Pelegrin P, Surprenant A. Pannexin-1 mediates large pore formation and interleukin-1beta release by the ATP-gated P2X7 receptor. EMBO J. 2006; 25:5071–5082. [PubMed: 17036048]

Penuela S, et al. Pannexin 1 and pannexin 3 are glycoproteins that exhibit many distinct characteristics from the connexin family of gap junction proteins. J Cell Sci. 2007; 120:3772–3783. [PubMed: 17925379]

Penuela S, Bhalla R, Nag K, Laird DW. Glycosylation regulates pannexin intermixing and cellular localization. Mol Biol Cell. 2009; 20:4313–4323. [PubMed: 19692571]

Penuela S, Gehi R, Laird DW. The biochemistry and function of pannexin channels. Biochim Biophys Acta. 2013; 1828:15–22. [PubMed: 22305965]

Qu Y, et al. Pannexin-1 is required for ATP release during apoptosis but not for inflammasome activation. J Immunol. 2011; 186:6553–6561. [PubMed: 21508259]

Sáez PJ, Shoji KF, Aguirre A, Sáez JC. Regulation of hemichannels and gap junction channels by cytokines in antigen-presenting cells. Mediators Inflamm. 2014; 2014:742734. [PubMed: 25301274]

Sandilos JK, Chiu YH, Chekeni FB, Armstrong AJ, Walk SF, Ravichandran KS, Bayliss DA. Pannexin 1, an ATP release channel, is activated by caspase cleavage of its pore-associated C-terminal autoinhibitory region. J Biol Chem. 2012; 287:11303–11311. [PubMed: 22311983]

Silverman WR, et al. The pannexin 1 channel activates the inflammasome in neurons and astrocytes. J Biol Chem. 2009; 284:18143–18151. [PubMed: 19416975]

Swayne LA, Sorbara CD, Bennett SA. Pannexin 2 is expressed by postnatal hippocampal neural progenitors and modulates neuronal commitment. J Biol Chem. 2010; 285:24977–24986. [PubMed: 20529862]

Thompson RJ, et al. Activation of pannexin-1 hemichannels augments aberrant bursting in the hippocampus. Science. 2008; 322:1555–1559. [PubMed: 19056988]

Vandesompele J, De Preter K, Pattyn F, Poppe B, Van Roy N, De Paepe A, Speleman F. Accurate normalization of real-time quantitative RT-PCR data by geometric averaging of multiple internal control genes. Genome Biol. 2002; 3:RESEARCH0034. [PubMed: 12184808]

Wang N. Paracrine signaling through plasma membrane hemichannels. Biochim Biophys Acta. 2013; 1828:35–50. [PubMed: 22796188]

Williams CD, et al. Role of the Nalp3 inflammasome in acetaminophen-induced sterile inflammation and liver injury. Toxicol Appl Pharmacol. 2011; 252:289–297. [PubMed: 21396389]

Williams CD, Bajt ML, Farhood A, Jaeschke H. Acetaminophen-induced hepatic neutrophil accumulation and inflammatory liver injury in CD18-deficient mice. Liver Int. 2010a; 30:1280–1292. [PubMed: 20500806]

Williams CD, Bajt ML, Sharpe MR, McGill MR, Farhood A, Jaeschke H. Neutrophil activation during acetaminophen hepatotoxicity and repair in mice and humans. Toxicol Appl Pharmacol. 2014; 275:122–133. [PubMed: 24440789]

Williams CD, Farhood A, Jaeschke H. Role of caspase-1 and interleukin-1beta in acetaminophen-induced hepatic inflammation and liver injury. Toxicol Appl Pharmacol. 2010b; 247:169–178. [PubMed: 20637792]

Xiao F, Waldrop SL, Khimji AK, Kilic G. Pannexin1 contributes to pathophysiological ATP release in lipoapoptosis induced by saturated free fatty acids in liver cells. Am J Physiol Cell Physiol. 2012; 303:1034–1044.

Europe PMC Funders Author Manuscripts

Europe PMC Funders Author Manuscripts

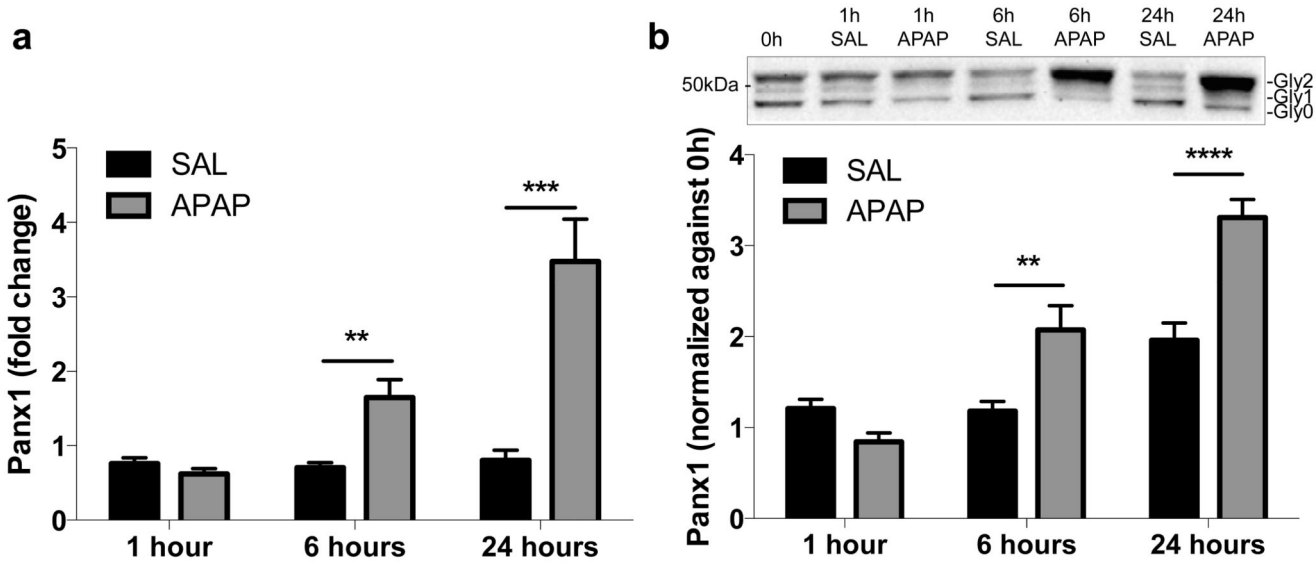

Figure 1. APAP overdosing induces hepatic RNA and protein expression of Panx1.

Mice (n = 5 per group and per time point) were injected 300 mg/kg APAP or saline (SAL) followed by sampling at different time points (0, 1, 6 and 24 hours). (a) RNA was extracted and subjected to RT-qPCR analysis of Panx1 using the primers as depicted in Table 1. Relative alterations in RNA levels were calculated according to the $2^{-\Delta\Delta Cq}$ formula, where the average expression of untreated animals at the 0 hour time point is set to 1. (b) Hepatic protein levels of Panx1 were assessed by immunoblot analysis, normalized against the total protein content and expressed as relative alteration compared to untreated animals. Data were expressed as means ± SEM, with $^{**}p < 0.01$, $^{***}p < 0.001$ and $^{****}p < 0.0001$ compared to vehicle control at indicated time points.

Europe PMC Funders Author Manuscripts
Europe PMC Funders Author Manuscripts

Europe PMC Funders Author Manuscripts

Europe PMC Funders Author Manuscripts

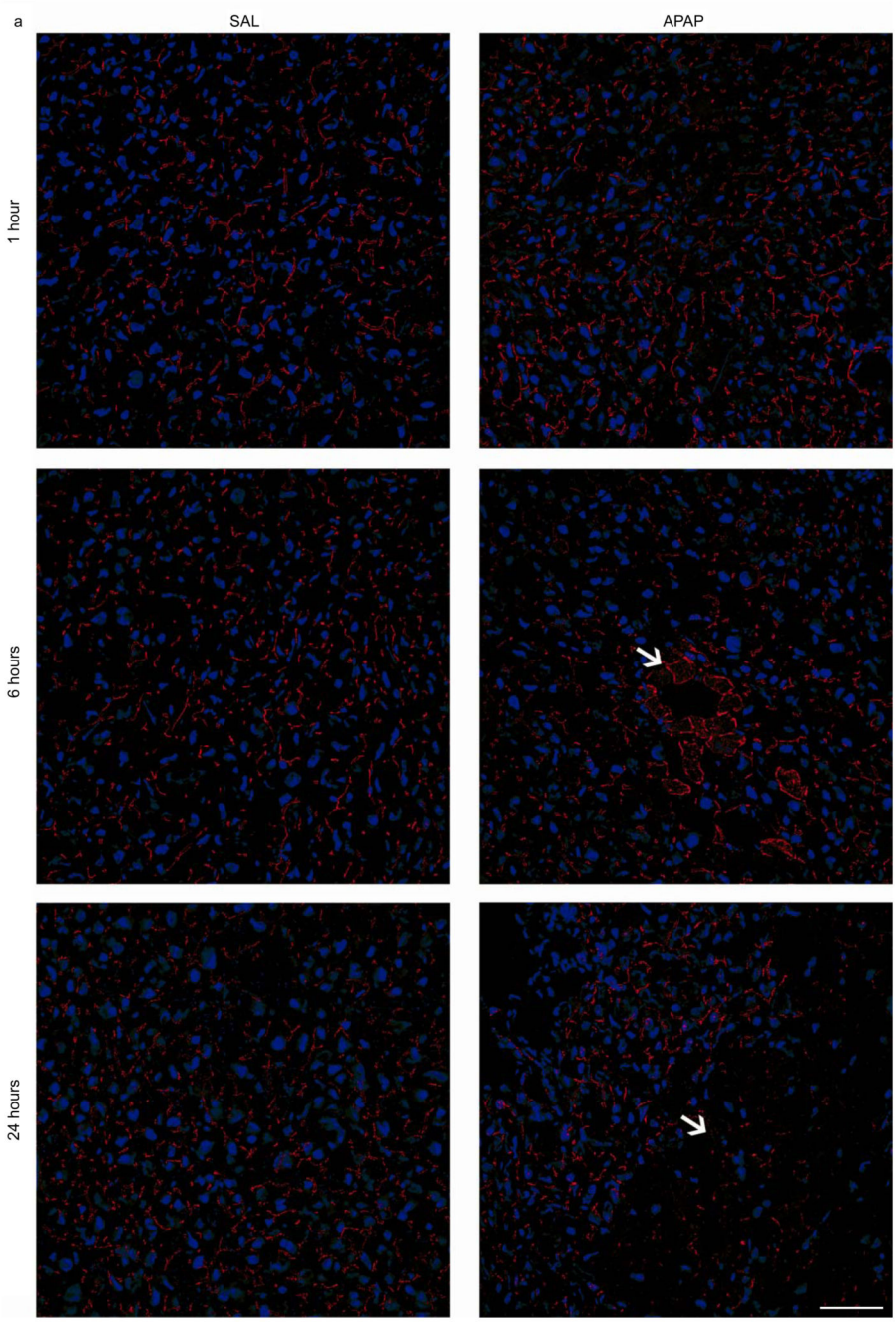

Europe PMC Funders Author Manuscripts

Europe PMC Funders Author Manuscripts

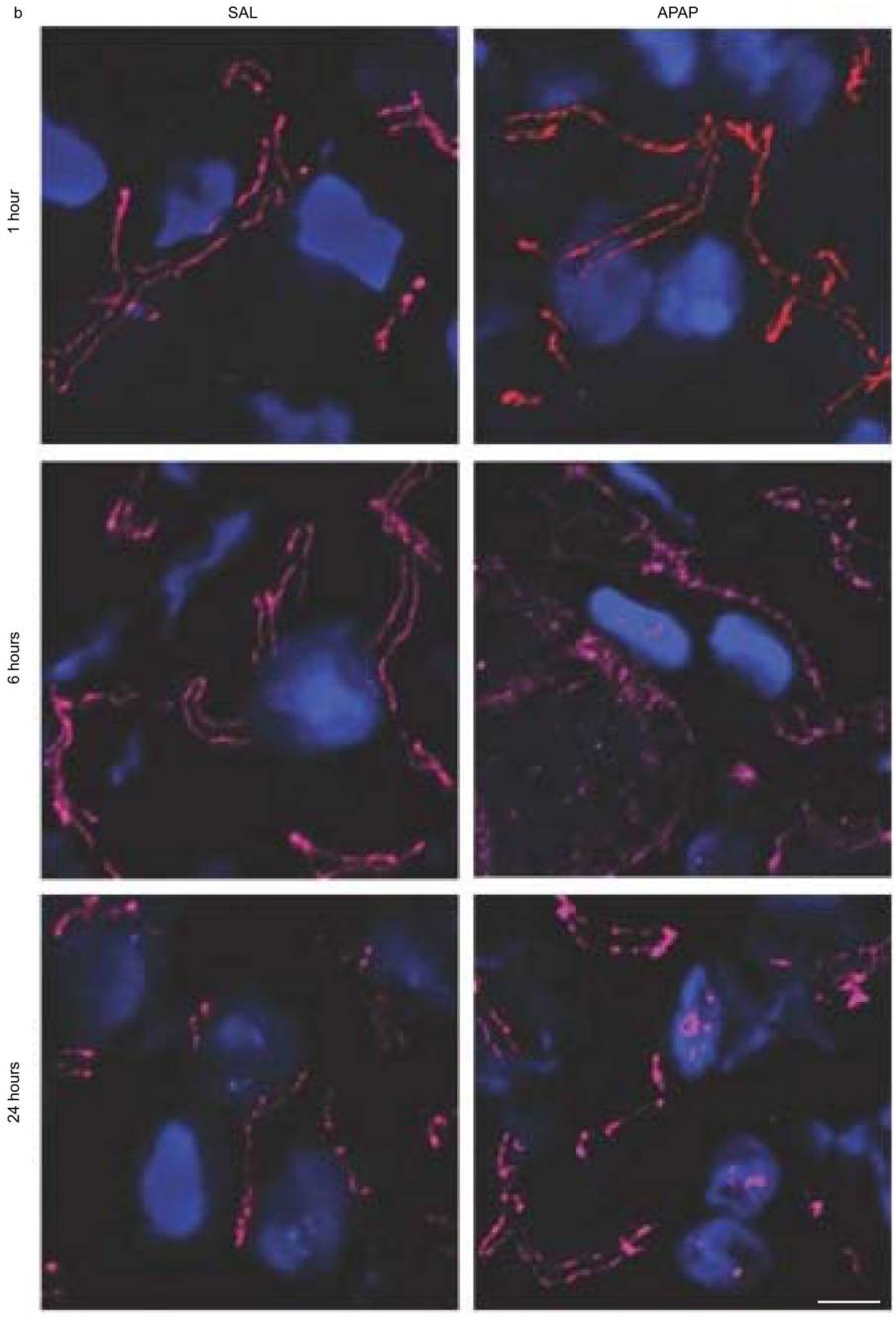

Figure 2. Alteration of hepatic Panx1 localization after APAP overdosing.

Mice (n = 5 per group and per time point) were injected with 300 mg/kg APAP or saline (SAL) followed by sampling at different time points (0, 1, 6 and 24 hours). Hepatic localization of Panx1 (red color) was assessed by immunohistochemical analysis on 10 μm liver sections fixed in acetone, which was merged with nuclear propidium iodide (blue color). The white scale bars represent (a) 50 μm and (b) 5 μm. The necrotic areas were pointed with white arrows.

Europe PMC Funders Author Manuscripts

Europe PMC Funders Author Manuscripts

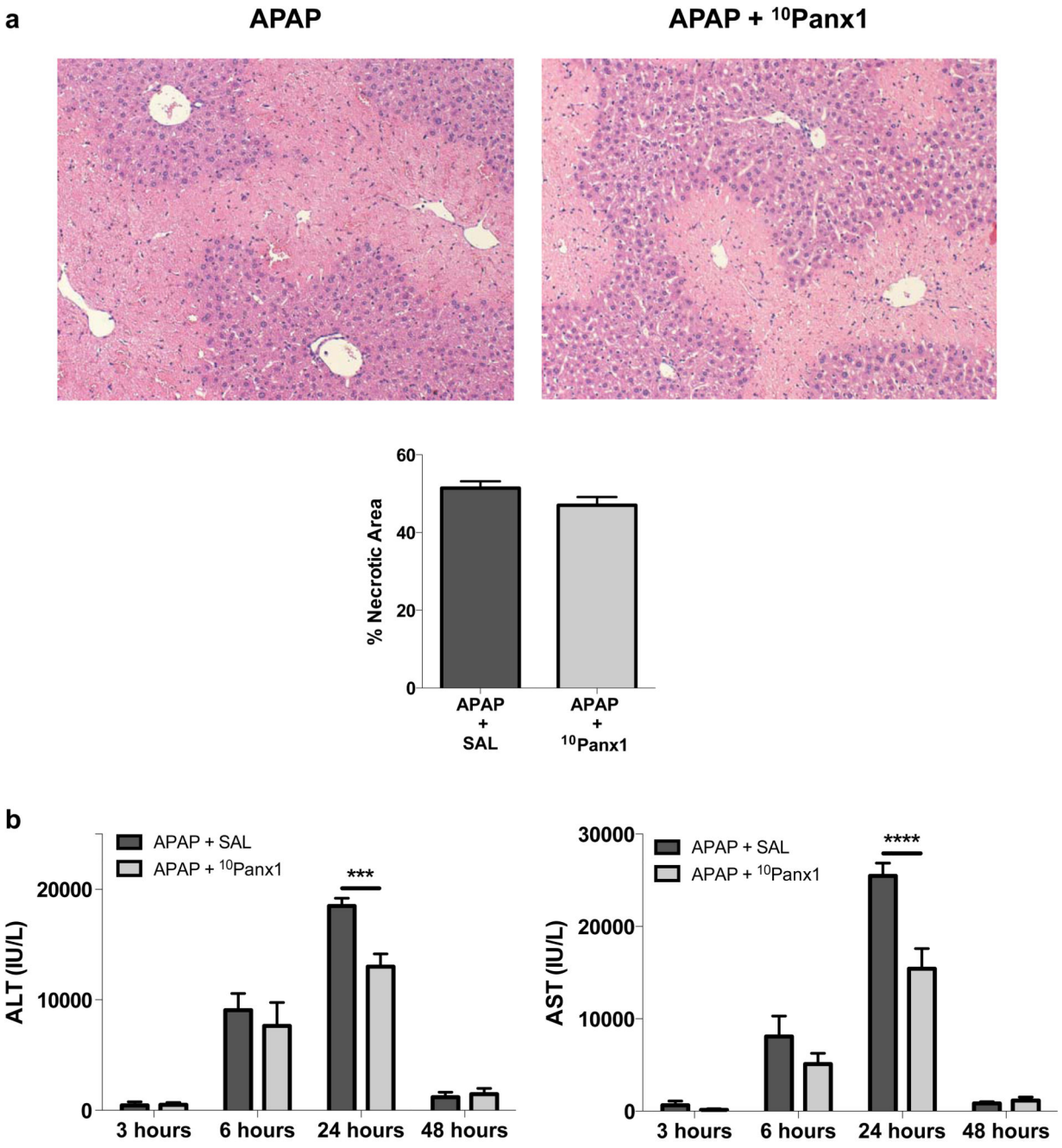

Figure 3. Panx1 channel inhibition diminishes cell injury following APAP overdosing.

Mice (n = 5 per group for 3 and 48 hours time points; n = 7 per group for 6 hours time point; n = 23 per group for 24 hours time point) were injected 300 mg/kg APAP or vehicle control followed by administration of 10 mg/kg ^{10}Panx1 or saline 1.5 hours later. Sampling was performed 3, 6, 24 and 48 hours after APAP overdosing. (a) Liver sections were examined microscopically after hematoxylin/eosin staining (100x magnification) (upper panel) with quantification of necrotic areas (lower panel) around the central veins at the 24 hours time point. (b) Serum levels of ALT (left panel) and AST (right panel). Data are expressed as

means ± SEM, with ***$p < 0.001$ and ****$p < 0.0001$ compared to APAP followed by vehicle administration.

Europe PMC Funders Author Manuscripts

Europe PMC Funders Author Manuscripts

Europe PMC Funders Author Manuscripts

Europe PMC Funders Author Manuscripts

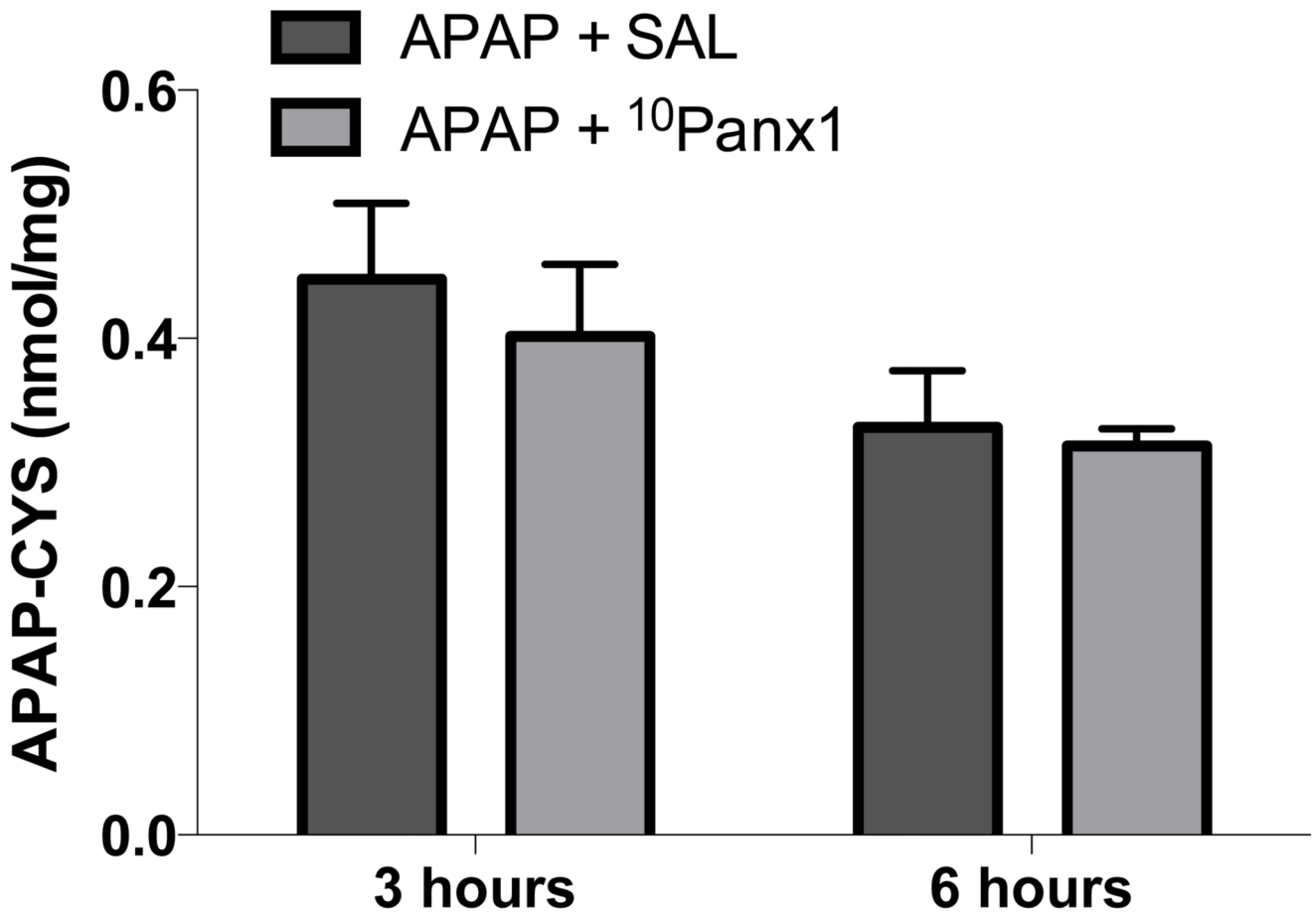

Figure 4. Panx1 channel inhibition does not affect hepatic protein adduct formation following APAP overdosing.

Mice (n = 5 per group and per time point) were injected 300 mg/kg APAP followed by administration of 10 mg/kg ^{10}Panx1 or saline (SAL) 1.5 hours later. Sampling was performed 3 and 6 hours after APAP overdosing. The generation of reactive metabolite results in the formation of APAP-cysteine (APAP-CYS) protein adducts, which were quantified by high-pressure liquid chromatography with electrochemical detection using total liver homogenate. Data are expressed as means ± SEM. No significant differences were found between mice treated with ^{10}Panx1 or vehicle control.

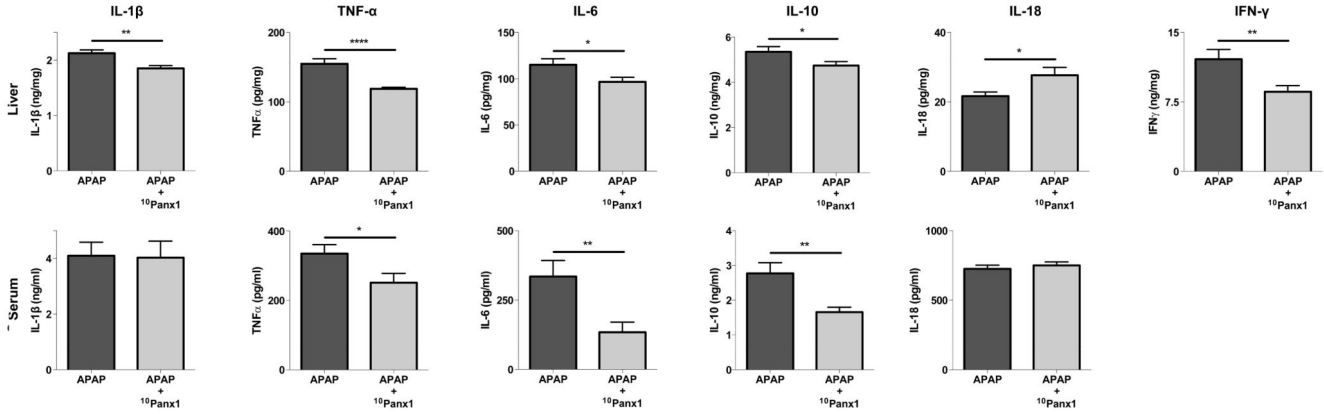

Figure 5. Panx1 channel inhibition differentially affects serum and liver cytokine levels following APAP overdosing.

Mice (n = 22 per group and per time point) were injected 300 mg/kg APAP followed by administration of 10 mg/kg ^{10}Panx1 or saline 1.5 hours later. Sampling was performed 24 hours after APAP overdosing. ELISA analysis of IL-1β, IL-6, IL-10, IL-18, TNFα and IFNγ were performed of liver (upper panels) and serum (lower panels) samples. Data are expressed as means ± SEM, with $*p < 0.05$, $**p < 0.01$ and $****p < 0.0001$ compared to APAP followed by vehicle administration.

Europe PMC Funders Author Manuscripts
Europe PMC Funders Author Manuscripts

Europe PMC Funders Author Manuscripts

Europe PMC Funders Author Manuscripts

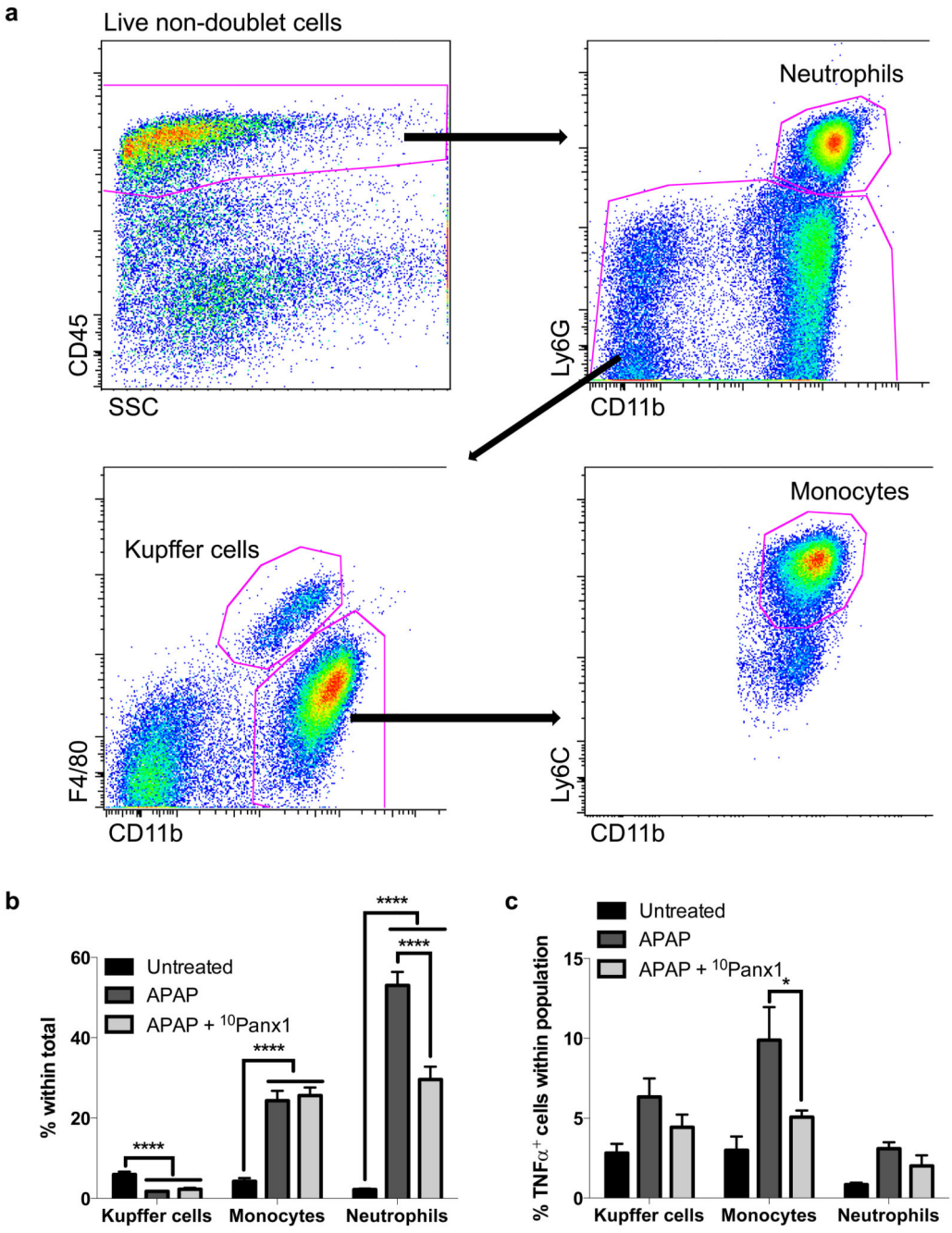

Figure 6. Panx1 channel inhibition reduces recruitment of neutrophils following APAP overdosing.

Mice (n = 8 for the untreated animals; n = 14 per group APAP-treated animals) were injected 300 mg/kg APAP followed by administration of 10 mg/kg ^{10}Panx1 1.5 hours later. Sampling was performed 24 hours after APAP overdosing. (a) Livers were subjected to flow cytometric analysis, where living, non-doublet cells were selected by forward and side scatter, out of which all CD45^{+} cells were included. From this, the neutrophils were detected as CD45^{+}CD11b^{hi}Ly6G^{+} cells, while Kupffer cells were selected as CD45^{+}Ly6G^{-}F4/80^{hi}CD11b^{int} cells and inflammatory monocytes as

$CD45^{+}CD11b^{hi}Ly6C^{hi}F4/80^{lo}$ cells. (b) Infiltration of Kupffer cells, inflammatory monocytes and neutrophils in untreated and APAP-overdosed animals whether or not treated with ^{10}Panx1, illustrated as percentage of the total living, non doublet cells. (c) Intracellular TNFα presence within each leukocyte population in untreated and APAP-overdosed animals whether or not treated with ^{10}Panx1. The percentage of TNFα-producing cells in the cell populations of interest was determined. Data are expressed as means ± SEM, with $*p < 0.05$ and $****p < 0.0001$.

Europe PMC Funders Author Manuscripts

Europe PMC Funders Author Manuscripts

Europe PMC Funders Author Manuscripts

Europe PMC Funders Author Manuscripts

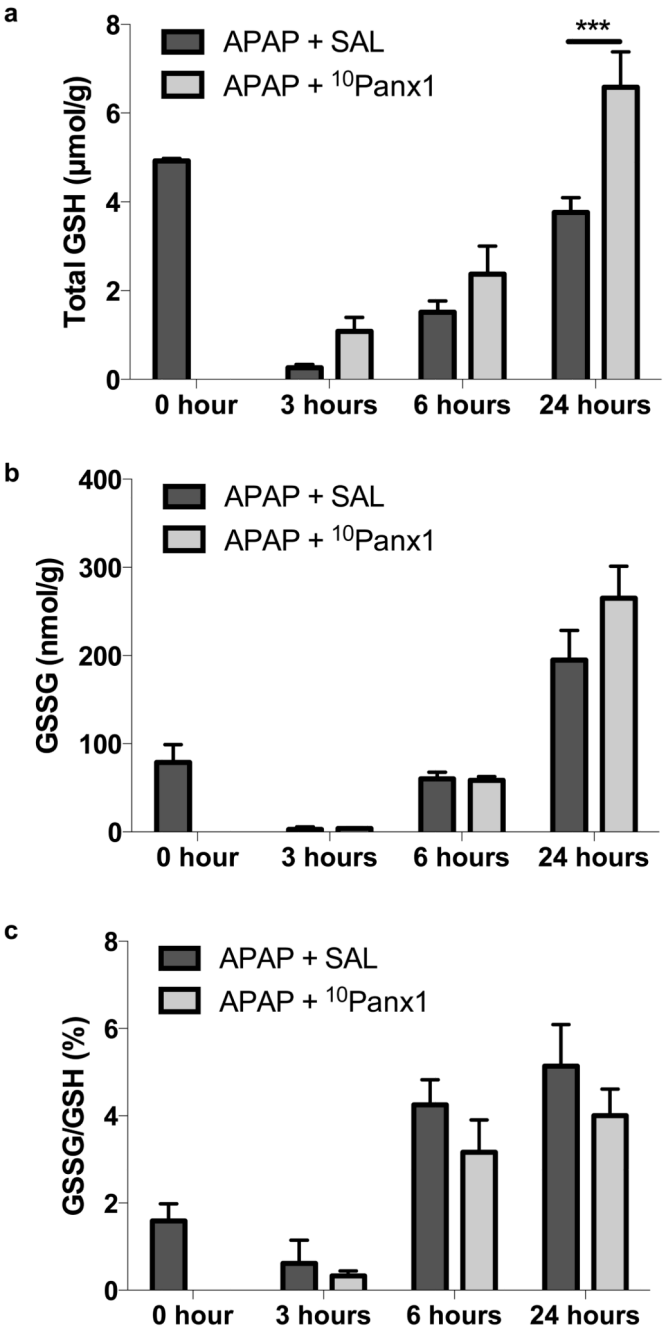

Figure 7. Panx1 channel inhibition alters the liver oxidative status following APAP overdosing.

Mice (n = 5 per group at 0, 3 and 6 hours time points; n = 12 per group for the 24 hours time point) were injected 300 mg/kg APAP followed by administration of 10 mg/kg ^{10}Panx1 or saline (SAL) 1.5 hours later. Sampling was performed 0, 3, 6 and 24 hours after APAP overdosing. Hepatic levels of (a) GSH and (b) GSSG were measured and (c) the GSSG/GSH ratio was calculated. Data are expressed as means ± SEM, with ***$p < 0.001$ compared to APAP followed by vehicle administration.

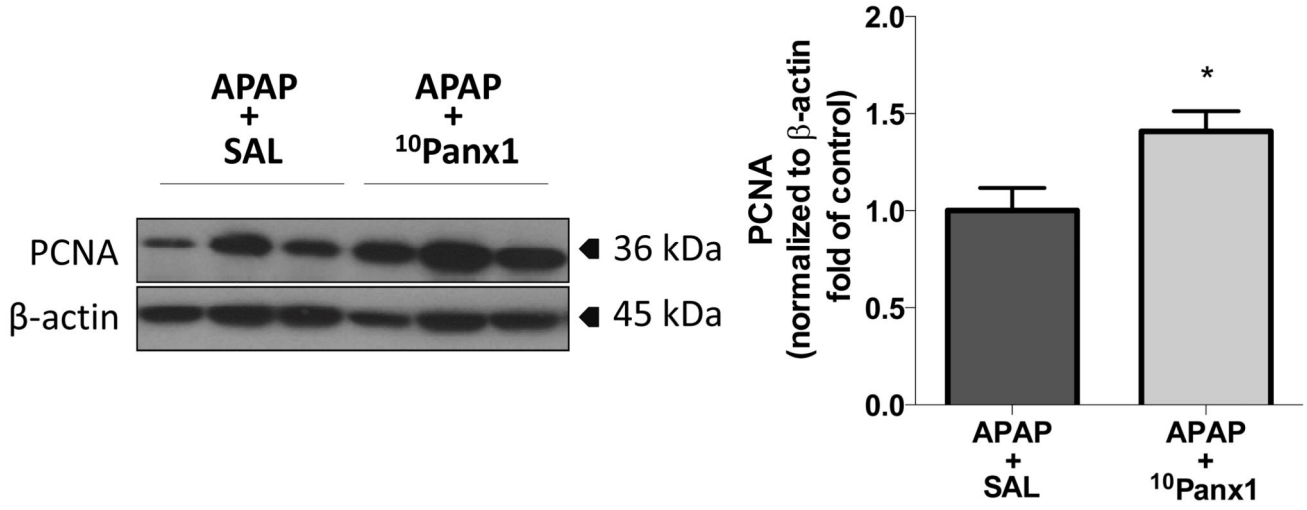

Figure 8. Panx1 channel inhibition promotes liver regeneration following APAP overdosing.

Mice (n = 10 per group) were injected 300 mg/kg APAP followed by administration of 10 mg/kg ^{10}Panx1 or saline (SAL) 1.5 hours later. Sampling was performed 24 hours after APAP overdosing. Hepatic protein levels of PCNA were assessed by immunoblot analysis and expressed as relative alteration compared to APAP-treated animals followed by SAL administration. Data are expressed as means ± SEM, with *$p < 0.05$ compared to APAP followed by vehicle administration.

Europe PMC Funders Author Manuscripts
Europe PMC Funders Author Manuscripts

Europe PMC Funders Author Manuscripts

Europe PMC Funders Author Manuscripts

Table 1

Primers used for RT-qPCR analysis.

Gene	Assay ID	Accession number	Assay location	Amplicon size (base pairs)	Exon boundary
Panx1	Mm00450900_m1	NM_019482.2	986	70	3-4
18S	Hs99999901_s1	X03205.1	604	187	1-1
Actb	Mm00607939_s1	NM_007393.3	1233	115	6-6
B2m	Mm00437762_m1	NM_009735.3	111	77	1-2
Gapdh	Mm99999915_g1	NM_008084.2	265	107	2-3
Hmbs	Mm01143545_m1	NM_013551.2	473	81	6-7
Ubc	Mm02525934_g1	NM_019639.4	370	176	2-2

Assay identification (ID) and accession number of target genes are indicated (18S, 18S ribosomal RNA; Actb, β-actin; B2m, β-2-microglobulin; Gapdh, glyceraldehyde 3-phosphate dehydrogenase; Hmbs, hydroxymethylbilane synthase; Panx1, pannexin1; Ubc, ubiquitin C).

Europe PMC Funders Author Manuscripts

Europe PMC Funders Author Manuscripts

Table 2
Panx1 glycosylation status after APAP overdosing.

Time point	Treatment	Total Panx1 normalized to 0 hour	Gly0 (%)	Gly1 (%)	Gly2 (%)
0 hour	/	1.00 ± 0.14	49.5 ± 1.4	13.9 ± 1.9	36.6 ± 3.3
1 hour	SAL	1.21 ± 0.10	58.6 ± 2.0	14.0 ± 1.9	27.3 ± 3.0
	APAP	0.85 ± 0.10	48.8 ± 3.5	5.2 ± 1.7***	46.0 ± 4.2**
6 hours	SAL	1.18 ± 0.11	54.1 ± 1.6	10.4 ± 1.3	35.6 ± 2.4
	APAP	2.08 ± 0.27	11.4 ± 5.7****	4.0 ± 1.0*	84.5 ± 6.6****
24 hours	SAL	1.96 ± 0.19	63.0 ± 1.8	18.1 ± 1.7	18.8 ± 0.7
	APAP	3.31 ± 0.20	5.7 ± 1.8****	3.8 ± 0.3****	90.5 ± 1.9****

Mice (n = 5) were injected 300 mg/kg APAP or saline (SAL) followed by sampling at different time points (0, 1, 6 and 24 hours). Hepatic protein levels of Panx1 were assessed by immunoblot analysis where Panx1 was detected as 3 signals, representing the non-glycosylated core (Gly0), the high-mannose (Gly1) and the complex glycosylated species (Gly2). Data were expressed as means ± SEM, with *$p < 0.05$, **$p < 0.01$, ***$p < 0.001$ and ****$p < 0.0001$ compared to vehicle control at indicated time points.